ESTIMATION OF DYNAMIC DISPLACEMENT OF GRAVITY TYPE QUAY WALLS BASED ON CENTRIFUGE MODELING

Tadafumi FUJIWARA[1], Kenichi HORIKOSHI[2], Yuichi HIGUCHI[3] And Toru SUEOKA[4]

SUMMARY

In recent years, when discussing stability of gravity type quay walls subjected to the so-called "Level 2" earthquakes, the design concept has been changed into one that focuses on an evaluation of performance. Under this new concept a certain amount of displacement is permitted as long as the functionality is maintained. Such an approach requires an accurate estimation of the displacement of gravity type walls during earthquakes. As a simple method for predicting displacement, the Newmark sliding block analysis is regarded as one of the most suitable methods. In this method, acceleration and external forces are applied from time to time to the structure which is modeled by a single mass system. Even though the Newmark method is considered to be quite effective, there is still a need to be improved for estimating the displacement of gravity type quay walls under huge seismic motions such as those observed in the 1995 Hanshin Awaji earthquake.

This paper presents the results of a series of dynamic centrifuge tests on earth pressure acting on quay walls, as well as a proposal of dynamic earth pressure model. Then, the proposed model was incorporated to the Newmark method in predicting quay wall displacements during earthquakes. The numerical results were compared with results from the centrifuge tests. The results showed that Westergaard's dynamic earth pressure yields accurate earth pressure of liquefied soil. It was also found that for a more accurate estimation of displacement, additional considerations of the frictional resistance beneath the wall and earth pressure during the liquefying process are necessary.

INTRODUCTION

Since the 1995 Hanshin Awaji earthquake, which caused large-scale displacements of quay walls surrounding reclaimed islands (Hamada et al, 1995) of Kobe city, a number of studies on the dynamic behavior of gravity type quay walls (in particular, the behavior under "Level 2" earthquakes) have been undertaken. In the conventional stability design of gravity type quay walls, any amount of displacement during and after earthquakes was not allowed. However, such a design concept is uneconomical and unrealistic for large earthquakes, and it is more rational to allow a certain amount of displacement (up to an acceptable level)

[1] *Taisei Research Institute, Taisei Corporation, Yokohama, Japan. Email: tadafumi.fujiwara@sakura.taisei.co.jp*
[2] *Taisei Research Institute, Taisei Corporation, Yokohama, Japan.Email: kenichi.horikoshi@sakura.taisei.co.jp*
[3] *Taisei Research Institute, Taisei Corporation, Yokohama, Japan.Email: yuichi.higuchi@sakura.taisei.co.jp*
[4] *Taisei Research Institute, Taisei Corporation, Yokohama, Japan.Email:toru.sueoka@sakura.taisei.co.jp*

considering its functions (for example, see Richards et al., 1979). Therefore, it now becomes more necessary than before to estimate the displacement of gravity type structures during earthquakes accurately.

Among a number of methods for estimating quay wall displacements during earthquakes, including effective stress analysis and empirical approaches based on observations of actual quay wall displacements. The Newmark sliding block analysis (Newmark, 1965) is regarded by many as one of simple and effective methods. In the method, acceleration and external forces are applied from time to time to the structure which is reduced to a single mass system. However, the Newmark method still has a need to be improved by taking into account the earth pressure during large wall displacements and the effects of soil liquefaction behind the wall.

Practically, the "Mononobe-Okabe method" (Okabe, 1924) has been used for the estimation of dynamic earth pressures acting on walls. However, it is fully accepted that this method can not be applied to calculate the pressure under high seismic intensity especially when the soil behind the wall liquefies.

The objective of this study is to establish a rational and simple design method for estimating the dynamic displacement of gravity type quay walls subjected to earthquakes. The authors first conducted a series of dynamic centrifuge tests to examine the earth pressure acting on quay walls and the quay wall displacement. In the tests, the effects of soil liquefaction on the displacement was also considered. Then, the observed earth pressures were compared with those conventionally fed to numerical analyses, and modeled to improve the Newmark method. The analytical results were compared with those from the centrifuge test results.

CENTRIFUGE TESTS

Model Design:

A schematic view of the centrifuge package used in the tests is shown in Figure 1. In this study, a centrifugal acceleration of 30 g (where "g" denotes the Earth's gravity) was applied to the model. The length of the soil package was 940 mm, and its inside width 260 mm. In the model, a rubber damper was attached at one end of the box to minimize the effects of the rigid end wall. Toyoura sand was poured into the package whose relative density *Dr* before the shaking was 40 % and saturated with silicone oil with a viscosity 30 times higher than that of water, to satisfy the similarity rule in the dynamic centrifuge model.

The model gravity wall was 170 mm in height and 70 mm in width, each corresponding to a 5.1 m high, 2.1 m wide at prototype scale. Six earth pressure transducers with a diameter of 10 mm were installed in the back side of the model wall along a vertical line at an interval of 25 mm. A thin layer of Toyoura sand was glued to the surface of the rigid plate beneath the wall, which resulted in the coefficient of friction,μ=0.36, between the wall base and the rigid plate. A 50 Hz sinusoidal wave motion was applied in a direction parallel to the length of the model. The maximum accelerations were set at 3.1 g, 4.6 g, 9.2 g and 12.2 g at the model scale (corresponding to 100, 150, 300 and 400 cm/sec^2 (Gal) at prototype scale, respectively). In the tests, the following two were tested:

Case 1: Soil saturated with the fluid level set at the ground surface
Case 2: The fluid level set below the ground surface and soil contains a non-liquefied layer

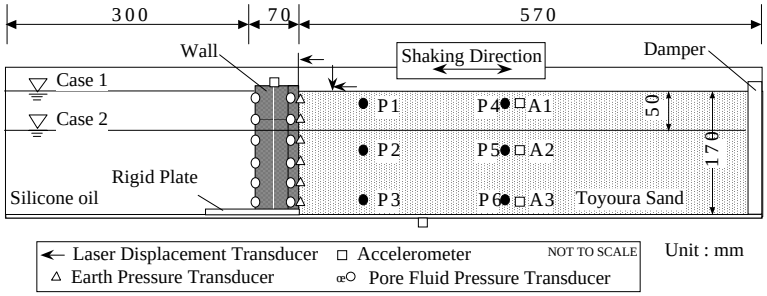

Figure 1: Schematic view of the centrifuge package

The design seismic intensity *kh*, which satisfies a safety factor *Fs* = 1.0 against sliding failure, was calculated as 0.13 for Case 1 and 0.15 for Case 2. The results of these tests were compared with those obtained from tests conducted earlier by the authors (Fujiwara et al. 1998) to examine the pressures acting on the wall and the effects of pore fluid on the behavior of the model wall.

Test results

Horizontal Displacement of Wall:

Time histories of the measured horizontal displacement are shown in Figures 2(a) and 2(b) (all results are shown at model scale unless otherwise specified). In all tests, the wall moved in the direction of the front side of the wall during shaking. In Case 1, the residual horizontal displacements at prototype scale were 205 mm at 100 Gal, 450 mm at 150 Gal, 740 mm at 300 Gal and 1140 mm at 400 Gal. In Case 2, the residual horizontal displacements at prototype scale were 135 mm at 100 Gal, 135 mm at 150 Gal, and 1250 mm at 400 Gal. At 300 Gal, since the displacement exceeded the capacity of the transducer so the measurement was not made. From the observation, horizontal displacements of the wall were considered to be divided into two components; (i) displacement due to the inertia force of the wall caused by the shaking and (ii) displacement due to the dynamic earth pressure.

In both Case 1 and Case 2, when an input motion of 100 Gal was applied, the wall continued to move even after the end of shaking. However, at higher accelerations of 150 Gal or more, the wall stopped immediately after the end of shaking. This difference in behavior is attributed to the value of negative pressure acting on the wall which resists to the wall motion. For the test of 100 Gal, it is deduced that the increase in total earth pressure as a result of increase in the positive pore fluid pressure made the displacement continue even after the shaking ended. On the other hand, at the higher accelerations of 150, 300 and 400 Gal, larger wall displacements led to the generation of negative pore fluid pressure, which prevented the wall from any further movement after the end of shaking.

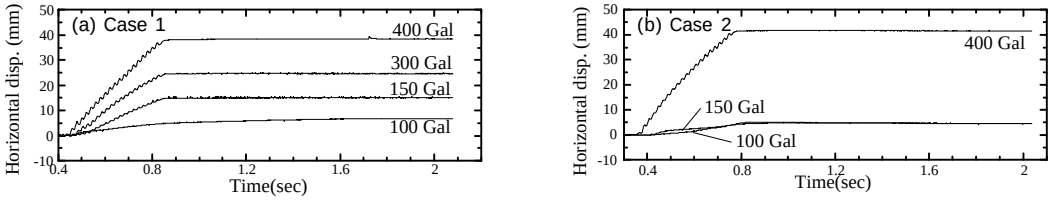

Figure 2: Horizontal displacement of wall

Figure 3 shows the relationship between input acceleration and residual horizontal displacement of the wall. In the figure, the results from dry soil case are also plotted after Fujiwara et al. (1998). The measured displacements were larger (in both Case 1 and Case 2) for saturated soil than those for dry soil. This was considered to be the results of (i) a higher earth pressure for the saturated soil condition than that for the dry soil condition, and (ii) a decrease in the apparent weight of the wall due to the effect of buoyancy. It was observed that the residual horizontal displacement became larger for input acceleration above the design seismic intensity of 0.13 for Case 1 and 0.15 for Case 2.

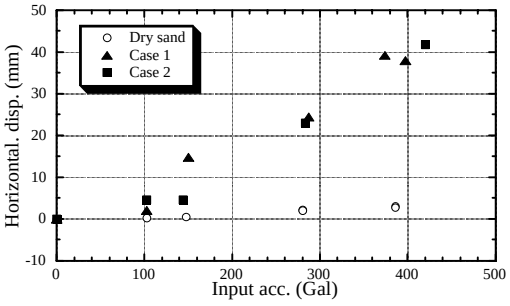

Figure 3: Relationship between input acceleration and residual horizontal displacement

Earth Pressure Acting on Wall:

Figures 4 and 5 show the time histories of total earth pressure acting on the wall at input accelerations of 100 Gal and 300 Gal (at prototype scale), respectively. At 300 Gal, total earth pressure increased at the beginning of shaking but soon afterwards started to decrease probably due to the influence of the wall movement. After the completion of shaking, total earth pressure did not immediately return to its initial value, but remained larger and gradually decreased. In Case 1, total earth pressure returned to its initial value a few minutes after the end of shaking, but in Case 2, its magnitude decreased to a value slightly larger than its initial value.

Comparing these observations with that for dry sand in which the earth pressure remained at a higher level after the end of shaking, the decrease of earth pressures in Cases 1 and 2 were seen to be affected by the dissipation of the excess pore fluid pressure.

The relationship between input acceleration and maximum effective earth pressure is shown in Figure 6 with earth pressure calculated using the Mononobe-Okabe method. The observed effective earth pressure in Case 1 was almost zero due to soil liquefaction, while those for the case of dry sand and Case 2 showed almost the same trends. In Case 1, the observed earth pressure agreed well with that calculated by the Mononobe-Okabe method. However, the measured values in Cases 1 and 2 did not agree with their corresponding computed values, especially for cases with high input motion. This discrepancy was thought to be arised from the fact that the Mononobe-Okabe method does not take into account the effects of soil liquefaction.

Total maximum earth pressure is also depicted in Figure 7 together with those estimated by the Mononobe-Okabe method. The measured values agreed only with calculated values for 300 Gal in Case 1, and were larger than calculated values for 100 Gal and 150 Gal. In the case of input accelerations over 300 Gal, the computed values are expected to be larger than measured values because of the use of the apparent seismic intensity (which was about 2 times higher than the actual seismic intensity) in the soil below the fluid level.

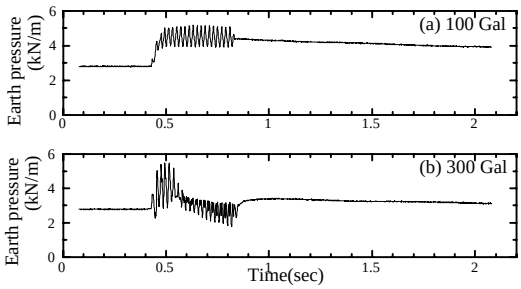

Figure 4: Total earth pressure (Case 1)

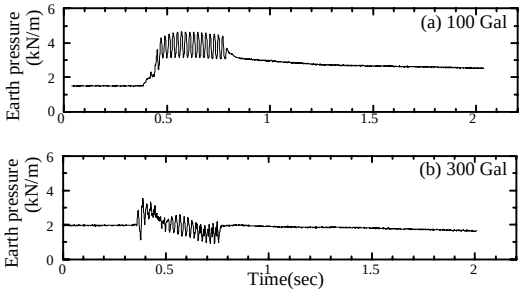

Figure 5: Total earth pressure (Case 2)

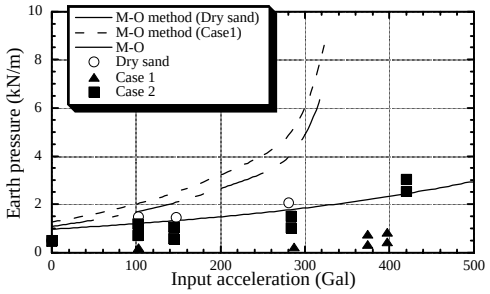

Figure 6: Total maximum effective pressure

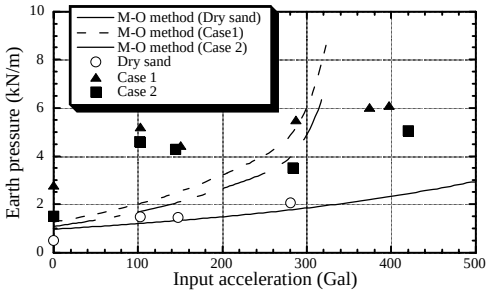

Figure 7: Total maximum earth pressure

INVESTIGATION OF EARTH PRESSURE MODEL

Earth Pressure Response:

Figures 8(a) to 8(d) summarize typical patterns of observed time histories of total earth pressure acting on the wall under four different conditions. Figure 8(a) shows the total earth pressure acting on the model wall submerged in silicone oil (for which case the observed pressure was equal to fluid pressure), showing that there was vibration only during shaking and the pressure returned to zero. For the case with dry sand, shown in Figure 8(b), total earth pressure increased gradually with vibration, and the residual value after the shaking was larger than its initial value.

Figure 8(c) shows the case when the input acceleration was relatively small for which the wall displacement was also small. The total earth pressure rapidly increased immediately after the start of shaking and decreased gradually after the completion of shaking. Figures 8(c) and 8(d) were obtained from the same model, the only difference is that in Figure 8(d) the wall undergoes a larger wall displacement. The total earth pressure in Figure 8(d) decreased rapidly some time after the start of the shaking due to the effect of negative fluid pressure caused by the large wall displacement.

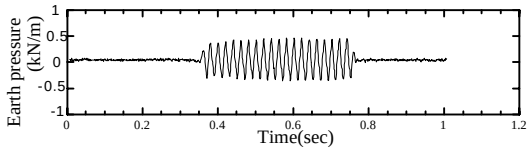

(a) Wall in silicone oil without backfill soil

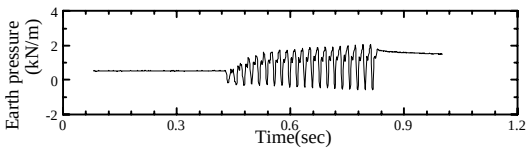

(b) Case with dry sand

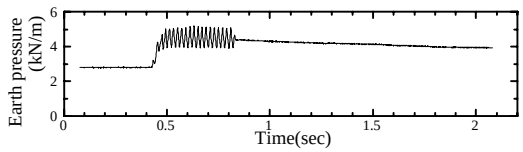

(c) Case with saturated sand (for small disp.)

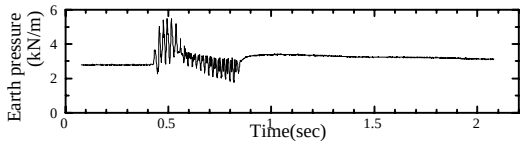

(d) Case with saturated sand (for large disp.)

Figure 8: Typical patterns of time histories of total earth pressure acting on wall

Modeling of Earth Pressure:

In this section, the patterns of total earth pressure increase are examined. Figure 9 illustrates a typical pattern of the observed time history of the total earth pressure. The time history can be divided into two components: the increase after the start of shaking (shown as component A in the figure) and the amplitude of the vibration component during shaking (shown as component B in the figure). The magnitude of components A and B have been compared in Figures 10 and 11, respectively. In Figure 10 for component A, the initial earth pressure increase was plotted, although some decrease was observed after some time. The zero input acceleration plot in Figure 10 corresponds to the initial value before shaking. In both figures, the results from the cases when the wall movement was restrained are added for comparison.

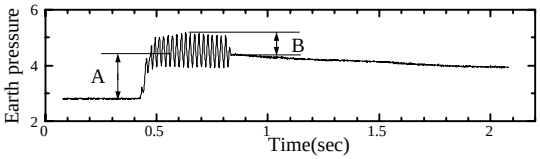

Figure 9: Deformation of components A and B

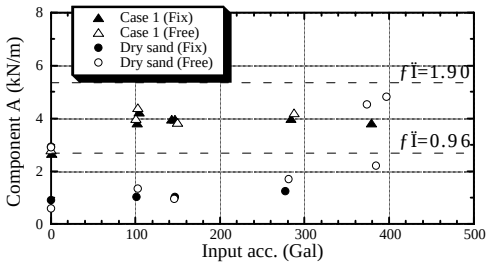

Figure 10: Component A of pressure

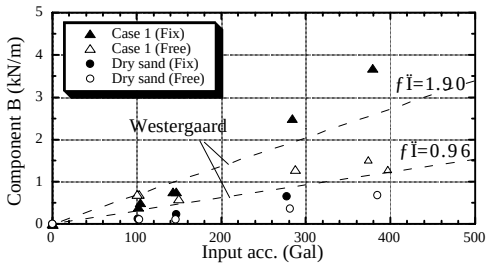

Figure 11: Component B of pressure

It is of interest that, in Figure 10, the magnitude of component A increased with input acceleration for dry sand while it remained constant for saturated sand irrespective of the magnitude of the input acceleration. The constant value corresponds to an earth pressure coefficient of $K = 0.7$. The constant earth pressure is due to soil liquefaction which was observed in all cases with saturated soil. The amplitude of component B depicted in Figure 11 showed an apparent increase with input acceleration for both dry sand and saturated sand. The magnitude of component B for saturated sand was seen to be larger than that for dry sand due to the effect of the wall displacement. The two broken lines in the figure show results obtained by the Westergaard equation using a fluid density of 0.96 t/m^3 (density of silicone oil) and 1.90 t/m^3 (wet density of saturated sand). The results described in this section is introduced to improve the simple method of estimating wall displacement during earthquakes which is referred to as the Newmark method.

ESTIMATION OF DYNAMIC DISPLACEMENT

Total Force Acting on Wall and Wall Displacement:

Figure 12 shows a schematic diagram of forces acting on a gravity type quay wall subjected to seismic motion. In the model, displacement of quay wall is governed by equilibrium between a resultant force (earth pressure, water pressure and inertia force) and frictional resistance acting on the wall base. Therefore, an evaluation of frictional force between the wall base and the ground becomes the key point in the estimation of displacement.

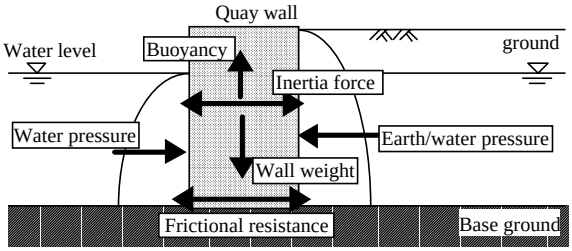

Figure 12: Schematic diagram of forces acting on a gravity type wall

Figure 13 shows the time history of resultant forces acting on a model wall and its horizontal displacement for the cases with input accelerations of 100 Gal and 300 Gal. The straight line in the figure shows the maximum static friction between the rigid plate and the model wall. It is evident from the figures that the model wall started to move not at the beginning of shaking but when the force acting on the wall exceeded the maximum static friction (as shown by the arrow in the figure).

For the case of input acceleration of 300 Gal, the displacement increased at a constant rate, as depicted in Figure 13(b), in spite of the remarkable drop in the resultant driving forces. This behavior indicates that the displacement during shaking was influenced much by the inertia force than by earth and fluid pressures. After the end of shaking, further displacement of the model wall, as was seen in the case at 100 Gal, was not observed when 300 Gal was applied.

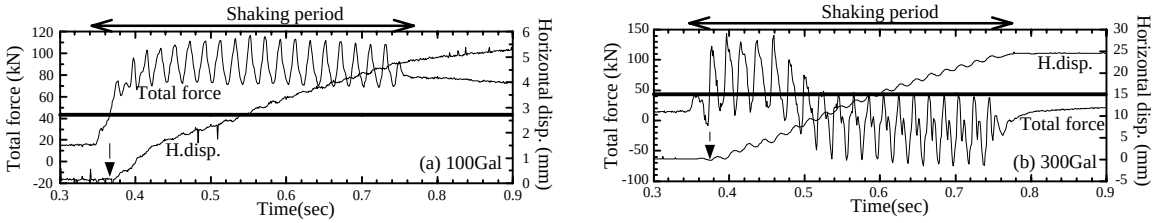

Figure 13: Time history of resultant forces acting on a wall and horizontal displacement.

Prediction of Dynamic Displacement

Newmark Method:

In this section, based on the results of the centrifuge tests, the quay wall sliding displacement during earthquakes was predicted by the Newmark method. In the method, the quay wall sliding behavior was expressed by a equilibrium between external forces such as earth pressure acting on the wall and frictional force acting on the quay wall base. Although the Newmark method is not able to deformation in the surrounding soil, this method generally requires fewer analytical parameters and shorter computation time, compared with more rigorous analyses such as finite element effective stress approaches.

As shown in Figure 14, the magnitude of sliding force was first calculated by evaluating the shear strength T at the bottom of the quay wall with earth/water pressure acting on the back of the wall and water pressure acting on the front. When T exceeds the frictional limit S_r, or when the quay wall has a relative velocity (as when the wall is sliding) in which case even if T is below S_r, the quay wall moved in accordance with the equation of motion. Water pressure acting on the front of the quay wall is obtained by summing up the "hydrostatic pressure P_{ws}" and "dynamic water pressure during earthquakes P_{wd}", while the earth pressure acting on the back of the walls

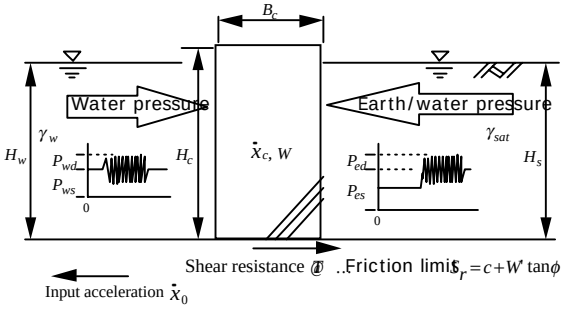

Figure 14: Analysis model of wall horizontal displacement

is obtained by the sum of "increase in earth pressure due to liquefaction P_{es}" and "dynamic earth pressure P_{ed}". Assuming that the soil at the back liquefied due to an increase in excess pore fluid pressure, both dynamic water pressure and dynamic earth pressure were calculated using the Westergaard equations. If soil and water near the wall did not move and only the wall moved during shaking, absolute acceleration of wall is used as the input acceleration for the Westergaard equations. However, when the model is shaking, the soil will be actually moving due to its shear modulus. It was therefore considered as more suitable to use a value in between the base acceleration and wall acceleration as the input acceleration in the Westergaard equations. Here, in the paper, the base acceleration was employed in place of the acceleration of the wall.

Results of Analyses:

The above method was applied to the centrifuge test cases with saturated soil in order to examine the applicability. Equations (1) and (2) were used to calculate the water pressure acting on the front wall, as these equations described the observed results well. On the other hand, the observed back earth pressures were explained by the following equations (3), (4), which introduced the factorsα and β, the computed values of back earth pressures were adjusted to the experimental values. The mean values of the factors α and β from the three cases were calculated as 0.87 and 0.60, respectively.

$$P_{ws} = \frac{1}{2}\gamma_w H_w^2 \quad \text{----- (1)} \qquad P_{wd} = -\frac{7}{12}\frac{\ddot{x}_0}{g}\gamma_w H_w^2 \quad \text{-----} \qquad (2)$$

$$P_{es} = \alpha\frac{1}{2}\gamma_{sat} H_s^2 \quad \text{----- (3)} \qquad P_{ed} = \beta\frac{7}{12}\frac{\ddot{x}_0}{g}\gamma_{sat} H_s^2 \quad \text{-----} \qquad (4)$$

The frictional coefficient, μ, acting on the base of the quay wall was measured as 0.36. However, the value of friction limit S_r in the centrifugal gravity field and in the presence of viscous fluid such as silicone oil is unknown. Therefore, in this paper S_r was assumed to be given by $S_r = c + \mu W'$, where c is a valiable.

Figure 15 shows the computed and observed quay wall displacements at prototype scale. The calculated wall displacement increased with an increase in input acceleration or a drop in c and the increase was greater when a smaller value for the friction limit of the quay wall base was fed. When c = 33.3 kN/m, the computed displacement became almost equal to the observed value. (In the case of c = 33.3 kN /m, it alternatively corresponds to a frictional angle of φ= 32°, assuming S_r is explained only by friction angle.) Figure 16 shows the time history of the wall displacement when c = 33.3 kN/m. It is clear from the figure that for the case of the input acceleration 300 Gal, the displacement developed step by step, showing a good agreement with the test results. The timing of the displacement increase, also, agreed well with the test results. The test results showed that the displacement curve slightly increased in a slight convex manner, whereas the computed sliding displacement showed more linear increase.

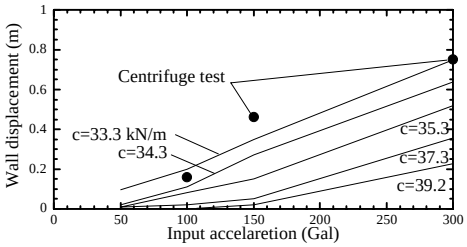

Figure 15: Input acceleration and horizontal displacement of wall

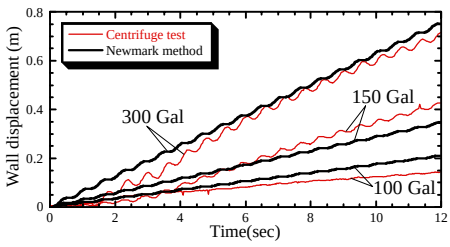

Figure 16: Time history of horizontal displacement of wall

The wall displacements computed by using the improved Newmark method are considered to be acceptable. However, further studies are required for modeling the base frictional resistance and the liquefaction pressure acting on the quay walls such as:

1. a more refined model of base frictional resistance,
2. modeling pressures for dynamic earth pressure and dynamic fluid pressure, including the effects of soil liquefaction as well as large wall displacement, and
3. modeling the effects of rotational and vertical displacement of the wall.

CONCLUSIONS

Based on the results from the centrifuge modeling of quay walls, an attempt was made to apply the so-called Newmark sliding block analysis to the evaluation of quay wall displacement subjected to huge earthquakes. It was found necessary to include the effects of soil liquefaction in the Newmark method. The results of the improved method were compared with the test results. The following main conclusions are drawn from this study:

1. Earth pressure and pore fluid pressure did not necessarily increase with input seismic intensity. However, they seemed to be, rather, highly influenced by the wall displacement.
2. The effective pressure acting on the wall during shaking dropped to almost zero with only a little variation depending on whether a non-liquefied layer was present or not.
3. The measured earth pressure acting on the wall agreed well with that predicted by the Mononobe-Okabe method for dry sand. However, as expected, the measured pressure with liquefied soil can not be explained by the Mononobe-Okabe method.
4. At the start of shaking, the model wall started to move when the resultant force acting on the wall exceeded the maximum static frictional resistance. However, during shaking the wall displacement seemed to be largely affected by the inertia force acting on it.
5. It was proposed to divide the total earth pressure response into two components: the initial increase and the subsequent vibration. The former component appeared to be constant for liquefied sand irrespective of the input motion. The latter component seemed to be proportional to the input motion even for liquefied sand conditions. This model incorporated in Newmark's sliding block analysis in devising a simple but effective method in predicting the wall displacement.

REFERENCES

1. Okabe, S. (1924), General Theory on Earth Pressure and Seismic Stability of Retaining Wall and Dam, Journal of Japan Society of Civil Engineers. Vol. 10, No. 6, pp. 1277-1323.
2. Newmark, N. M. (1965), Effects of Earthquakes on Dams and Embankments, Geotechnique, Vol.15, No. 2, pp. 139-159.
3. Richards, E. & Elms, D. (1979), Seismic Behavior of Gravity Retaining Walls, ASCE J. Geotechnical Eng. Div., Vol.10.5, No. GT.4.
4. Hamada, M., Isoyama, R., & Wakamatsu, K. (1995), The Hyogoken-Nanbu (Kobe) Earthquake, Liquefaction, Ground Displacement and Soil Condition in Hanshin Area, Association for Development of Earthquake Prediction, The School of Science and Engineering, Waseda University and Japan Engineering Consultants Co., Ltd.
5. Fujiwara, T., Horikoshi, K., & Sueoka, T. (1998), Dynamic Behavior of Gravity Type Quay Wall and Surrounding Soil During Earthquake. Proceeding of Centrifuge 98, Tokyo, pp. 359-364.